ELSEVIER

Journal of Power Sources 113 (2003) 124–130

JOURNAL OF POWER SOURCES

www.elsevier.com/locate/jpowsour

Structural considerations of intermetallic electrodes for lithium batteries☆

M.M. Thackeray[a,*], J.T. Vaughey[a], C.S. Johnson[a], A.J. Kropf[a], R. Benedek[a], L.M.L. Fransson[b], K. Edstrom[b]

[a]*Electrochemical Technology Program, Argonne National Laboratory, Chemical Technology Division, Argonne, IL 60439, USA*
[b]*Materials Chemistry, Ångström Laboratory, Uppsala University, Uppsala S-751 21, Sweden*

Received 10 July 2002; accepted 22 September 2002

Abstract

Although metal alloys and intermetallic compounds have been researched extensively as possible negative electrodes for lithium batteries, only recently have efforts been made to monitor the phase transitions that occur during their reaction with lithium by in situ X-ray diffraction. These studies have lead to attempts to exploit those systems that show strong structural relationships between a parent structure and its lithiated products. In this paper, an overview of several systems is presented, particularly those that operate by lithium insertion/metal displacement reactions with a host metal array at room temperature. An analogy between these reactions and the high-temperature electrochemical reaction of sodium/nickel chloride cells, which is 100% efficient, is provided. On this basis, a prognosis for using intermetallic electrodes in lithium-ion cells is given.

Keywords: Lithium batteries; Intermetallic electrode; Structure

1. Introduction

Considerable research has been undertaken over the past two to three decades to develop a viable lithium–metal alloy or lithium-intermetallic compound as the negative electrode for lithium batteries. Early efforts were placed on binary lithium-metal systems, Li_xM, such as Li_xAl, Li_xSb, Li_xSi and Li_xSn [1]. These electrodes are generally considered unsuitable because the structural changes and the anomalously large volume expansion that are associated with lithium insertion destroy the structural integrity of the electrode, thereby limiting the ability of the lithium cell to cycle with high efficiency. Greater success has been achieved with composite electrode structures, such as those derived from SnO [2,3], in which an active component, Li_xSn, can cycle within an inactive matrix, Li_2O, or those derived from $FeSn_2$ [4] or $CoSb_3$ [5] in which active Li_xSn and Li_3Sb cycle within inactive Fe and Co matrices, respectively. In these systems, the large structural differences that exist between the parent and lithiated compounds limit the reconstruction of the parent structure during delithiation. Furthermore, this approach has not yet overcome the large irreversible capacity loss that occurs when intermetallic electrodes are initially cycled. In a different approach to improve the reversibility of intermetallic electrodes, studies have been made of compounds such as SnSb [6,7], Cu_6Sn_5 [8,9], InSb [10–12], Cu_2Sb [13] and MnSb [14] that show strong structural relationships to their lithiated products.

In this paper, the structural changes that occur when metals and intermetallic compounds are lithiated are discussed in terms of various reaction types. Of particular importance are the reactions that occur by reversible lithium insertion/metal displacement reactions with a face-centered-cubic (fcc) host structure. Such reactions are characteristic of the electrochemical process that occurs at 300 °C in sodium/metal chloride "Zebra" cells:

$$2Na + MCl_2 \rightarrow 2NaCl + M \quad (1)$$

in which M = Fe, and/or Ni [15–17]. The strong similarity that exists between the high-temperature reaction (1), which is 100% efficient, and the room temperature reactions of lithium with some intermetallic compounds, such as Cu_2Sb, provides optimism for overcoming the current limitations of

☆This paper was presented, in part, at the 11th International Meeting on Lithium Batteries, Monterey, CA, USA, 24–28 June 2002.

* Corresponding author. Tel.: +1-630-252-9184; fax: +1-630-252-4176.
E-mail address: thackeray@cmt.anl.gov (M.M. Thackeray).

0378-7753/02/$ – see front matter
PII: S0378-7753(02)00538-4

intermetallic electrodes in lithium cells; a prognosis for overcoming these limitations is given.

2. The role of structure in electrochemical reactions

Structure plays an important role in the reversibility of electrochemical reactions, particularly those involving topochemical processes [18]. This is particularly true for layered $LiCoO_2$, $LiNiO_2$, and $LiMnO_2$ electrode structures, and the spinel $LiMn_2O_4$. In these examples, the reversibility and efficiency of the reaction is dependent on the compositional range over which lithium can be extracted from the electrode structure without damaging the structural integrity of the transition metal oxide framework, for example, either by internal atomic displacements or by reaction with the electrolyte at high potentials. Lithium insertion/extraction reactions with these metal oxides are accompanied by relatively small changes to the unit cell parameters and volume. This scenario does not exist with metals or intermetallic compounds, because their dense structures do not provide an energetically favorable interstitial space for additional lithium. The reactions of lithium with metals and intermetallic compounds, therefore, tend to be accompanied by a significant increase in crystallographic volume.

Lithium can react with metals, denoted A, and intermetallic compounds, for example binary systems, denoted AB, in various ways:

(i) by lithium insertion (addition) and an internal displacement of the atoms within a parent host structure:

$$x\mathrm{Li} + \mathrm{A} \rightarrow \mathrm{Li}_x\mathrm{A} \quad (2)$$

$$x\mathrm{Li} + \mathrm{AB} \rightarrow \mathrm{Li}_x\mathrm{AB} \quad (3)$$

(ii) by lithium insertion and substitution to form a ternary phase that may involve solid–solution behavior:

$$x\mathrm{Li} + \mathrm{AB} \rightarrow \mathrm{Li}_x\mathrm{A}_{1-y}\mathrm{B} + y\mathrm{A} \quad (4)$$

(iii) by lithium insertion and the complete displacement of one of the metals to yield a new binary phase:

$$x\mathrm{Li} + \mathrm{AB} \rightarrow \mathrm{Li}_x\mathrm{B} + \mathrm{A} \quad (5)$$

Examples of these reaction types are provided below:

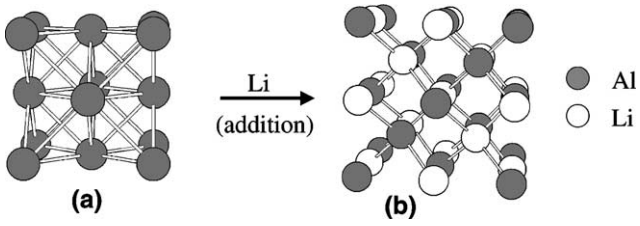

Fig. 1. The transition of (a) Al to (b) LiAl.

2.1. The reactions of Li with Al and Sb

Schematic illustrations of the phase transitions that occur when Li reacts with Al and Sb to yield LiAl and Li_3Sb are provided in Figs. 1 and 2, respectively; they are representative of reaction type (2). Although both aluminum (space group Fm3m) and its lithiated product LiAl (space group Fd3m) have fcc structures, the fcc array of the parent Al structure does not remain intact during the transformation to LiAl. In Al, all the atoms reside at fcc positions, whereas in LiAl 50% of the Al atoms occupy the fcc positions, while the remaining 50% occupy one-half of the tetrahedral interstices; the inserted Li atoms occupy the remaining tetrahedral interstices and all the octahedral interstices (Fig. 1). Therefore, this transition, which necessitates the diffusion of both Li and Al over significant distances, results in a major structural rearrangement of the Al lattice and a significant increase in unit cell volume (95% per Al atom).

Antimony metal has a distorted rocksalt structure with space group symmetry R-3m (Fig. 2). It can, therefore, be regarded as having two interpenetrating fcc Sb arrays. On full lithiation, the resulting product, Li_3Sb (Fm3m), has only one fcc Sb array in which the Li atoms occupy all the interstitial tetrahedral and octahedral sites. Like Al, the transition of Sb to Li_3Sb involves the addition of lithium and a significant internal displacement and rearrangement of 50% of the Sb atoms within the structure; the lattice expands by 137% per Sb atom (note: on slow electrochemical lithiation, an intermediate Li_2Sb structure is formed a few millivolts above the potential for the Sb to Li_3Sb transition [11].)

The significant atomic displacements, structural rearrangements and large volume increases that accompany lithium insertion into metals leads to electrochemical pulverization of the particles and the loss of electronic contact between them; these phenomena are generally believed to be among

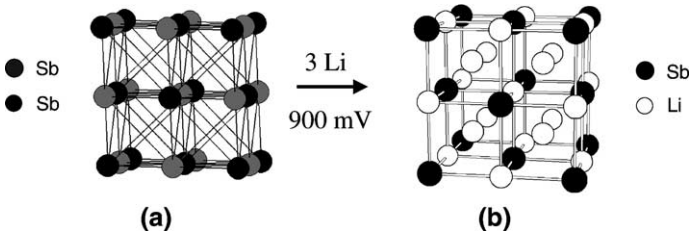

Fig. 2. The transition of (a) Sb to (b) Li_3Sb.

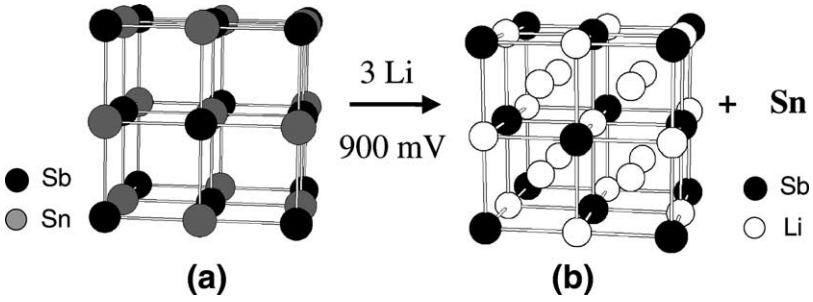

Fig. 3. The transition of (a) SnSb to (b) Li_3Sb.

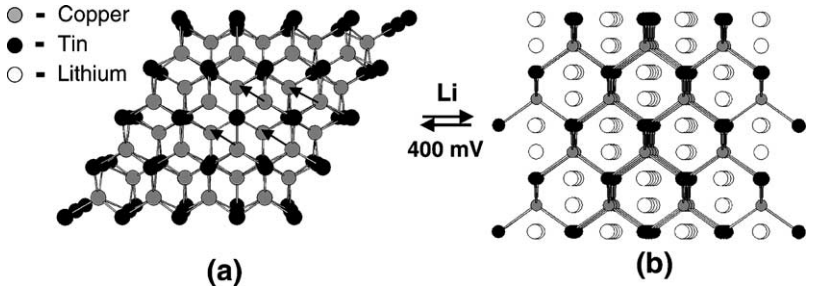

Fig. 4. The transition of (a) Cu_6Sn_5 to (b) Li_2CuSn. The interstitial Cu atoms in trigonal bipyramidal sites have been omitted for clarity.

the main reasons that limit the cycle life of metal electrodes in lithium cells [19].

2.2. The reaction of Li with SnSb

SnSb is isostructural with Sb but has an undistorted rocksalt structure (Fig. 3); it is cubic (space group Fm3m) with a lattice parameter $a = 5.880$ Å. Lithium reacts with SnSb at approximately 800 mV versus Li to form Li_3Sb ($a = 6.572$ Å) and metallic tin [3]; the reaction can be viewed simplistically as lithium insertion into, and tin displacement from, an Sb host structure (reaction type (5), Fig. 3). This process occurs predominantly at the surface of the electrode particles because it is accompanied by a large volume expansion, a concomitant extrusion of Sn and a significant reduction in particle size. Therefore, these reactions differ from conventional insertion reactions with metal oxides, which occur with relatively small volume changes, without metal extrusion, and without the same degree of pulverization. Unlike the reaction of lithium with Sb that requires a rearrangement of the Sb atoms, the Sb atoms in SnSb remain in their fcc positions during lithium insertion/tin extrusion; in the SnSb to Li_3Sb transformation, the volume expansion (per Sb atom) is only 40%, which is significantly less than it is for the Sb to Li_3Sb transition (137%); however, the electrode expands overall by 93%, when the extruded Sn is considered. This reaction is reversible [7], but it is dependent on the availability of extruded Sn atoms at the surface of the Li_3Sb particles. Lithiation of the extruded tin occurs at lower potentials to yield compounds in the Li_xSn system $(0 < x < 4.4)$, which increases the capacity of the electrode. These low voltage reactions, which result in further electrode expansion and a loss of interparticle contact between the Li_3Sb and Sn components, compromise the reversibility of the high voltage Li_3Sb to SnSb reaction [6].

2.3. The reaction of Li with Cu_6Sn_5

Cu_6Sn_5 has a NiAs-type structure (Fig. 4) in which one-sixth of the copper atoms reside in interstitial trigonal bipyramidal sites of the "CuSn" (NiAs) framework. Lithium reacts with Cu_6Sn_5 at approximately 400 mV to yield a lithiated zinc-blende structure Li_2CuSn [8]. The ideal reaction

$$10Li + Cu_6Sn_5 \rightarrow 5Li_2CuSn + Cu \quad (6)$$

occurs by a topotactic transformation[1] in which 50% of the Sn atoms in the NiAs framework are cooperatively displaced into neighboring trigonal bipyramidal sites, thereby dislodging the interstitial Cu atoms from these sites and extruding them from the structure. During the nickel–arsenide to zinc-blende transition, the remaining copper atoms (83%) and tin atoms (50%) maintain their orientation relationship (Fig. 4). This reaction is reversible but shows considerable hysteresis, which can be attributed to the relatively slow diffusion of Sn within the intermetallic host structure. Based on literature values for the crystallographic parameters of phase-pure Cu_6Sn_5 and Li_2CuSn,

[1] A topotactic transformation is defined by IUPAC as "a transition in which the crystal lattice of the product shows one or more crystallographically equivalent, orientational relationships to the crystal lattice of the parent phase" [20].

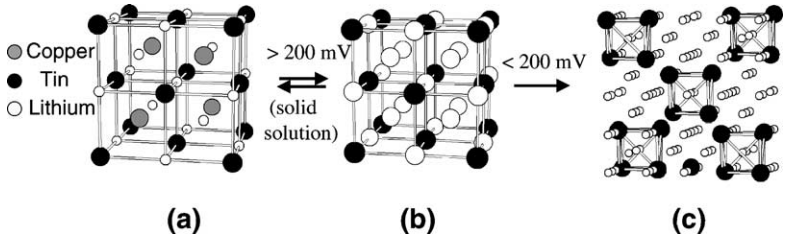

Fig. 5. The transition of (a) Li_2CuSn to (c) $Li_{4.4}Sn$ via hypothetical (b) "Li_3Sn".

the volumetric increase during the topotactic transformation is 57% per Sn atom.

Lithium can react further with Li_2CuSn. In situ X-ray diffraction data have shown that the reaction occurs first by substitution of Cu by Li, which results in a solid solution $Li_{2+x}Cu_{1-x}Sn$ for $0 < x < 1$ (reaction type (4)), and thereafter, once all the copper has been extruded at $x = 1$ "Li_3Sn", in the formation of $Li_{4.4}Sn$ (Fig. 5). No evidence has yet been seen in cycled electrodes of known intermediate Li_xSn phases, such as Li_7Sn_2, between Li_3Sn and $Li_{4.4}Sn$. Note, however, that "Li_3Sn" is not one of the known compositions in the lithium–tin system, and that it may be stabilized by a small amount of residual copper within the fcc structure before transforming to $Li_{4.4}Sn$. The Li_2CuSn to Li_3Sn transition, in which the fcc Sn array remains intact, is reversible but the degree of reversibility is dependent on the availability, size and close proximity of the extruded copper to the lithiated tin particles. Of particular note is that "Li_3Sn" units provide the building blocks for the $Li_{4.4}Sn$ structure (Fig. 5). During the Li_3Sn to $Li_{4.4}Sn$ transition, individual units of Li_3Sn are prised apart to accommodate additional lithium. This process destroys the structural integrity of the Sn array, thereby limiting the reconstruction of the fcc Sn array during charge and severely damaging the reversibility of the overall reaction. The overall volume expansion that accompanies a Cu_6Sn_5 to $Li_{4.4}Sn$ transition is 148% per Sn atom, and 184% if the extruded Cu extrusion is included in the calculation. This interpretation for the loss of capacity of Li/Cu_6Sn_5 cells is consistent with the capacity fade that depends on the voltage window during electrochemical cycling (Fig. 6). For example, when the Li/Cu_6Sn_5 cells are cycled between 1.2 and 0 V, i.e. between the stability limits of Cu_6Sn_5 and $Li_{4.4}Sn$, capacity is lost rapidly. However, by raising the lower voltage to 0.1 and 0.2 V, thereby restricting the structural changes to topotactic processes, a significant improvement in cycling efficiency can be achieved, albeit at the expense of capacity [8].

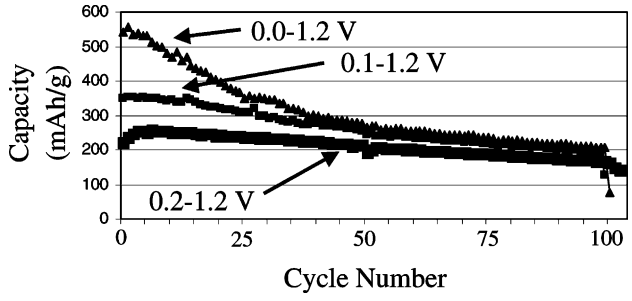

Fig. 6. Capacity versus cycle no. for Li/Cu_6Sn_5 cells (0.2 mA/cm^2).

2.4. The reaction of Li with MnSb

Unlike Cu_6Sn_5, MnSb has the ideal NiAs composition and structural configuration. Therefore, during the initial reaction, lithium can be inserted into the MnSb structure with a concomitant displacement of 50% of the Sb atoms into neighboring interstitial sites to generate an fcc Sb array, without the extrusion of any Mn atoms. The transformation is representative of reaction type (3). In this case, however, only one Li atom is introduced per MnSb unit; the product is LiMnSb with an ordered antifluorite-type structure, in which the Li and Mn atoms occupy all the tetrahedral sites of the Sb array [14]. The volume expansion for this reaction is 49% per Sb atom. A mechanism for this reaction has been proposed in which lithium insertion is accompanied by the displacement of the Sb atoms to yield an intermediate MnSb zinc-blende framework (similar to the Cu_6Sn_5 to Li_2CuSn transition) that induces a simultaneous displacement of one-half of the Mn atoms in the unit cell into neighboring vacant tetrahedral sites to create the layered MnSb framework of the LiMnSb structure (Fig. 7). Further insertion of lithium into LiMnSb displaces the Mn atoms from the lattice to yield Li_3Sb in which the lithium atoms occupy all the tetrahedral and octahedral sites of the fcc Sb array; some solid solution behavior has been observed between LiMnSb and Li_3Sb [14]. The reactions are rever-

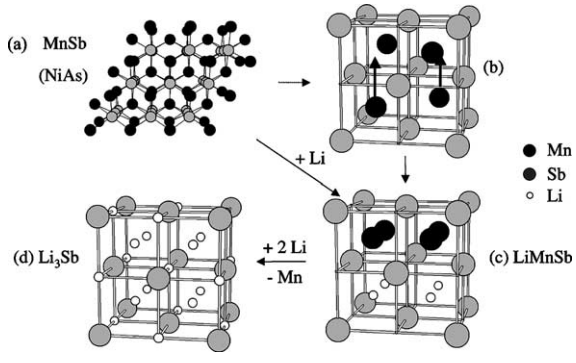

Fig. 7. The transition of (a) MnSb to (d) Li_3Sb via (c) LiMnSb. The proposed transformation of (a) MnSb (NiAs framework) to (c) LiMnSb occurs through (b) an intermediate zinc-blende MnSb framework.

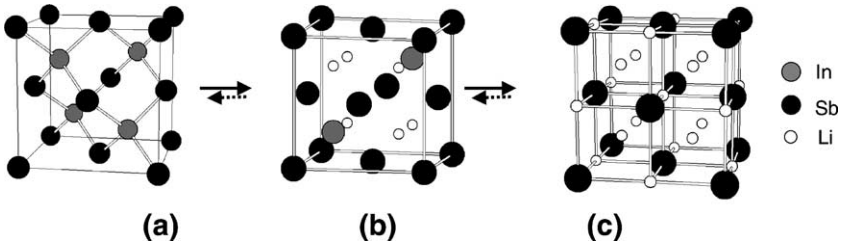

Fig. 8. The transition of (a) InSb to (b) Li_3Sb via hypothetical (b) "$Li_{1.5}In_{0.5}Sb$".

sible; the total expansion of the electrode on complete lithiation, including the extruded Mn, is 96%.

The hysteresis that occurs during the topotactic transformation of NiAs-type structures, such as Cu_6Sn_5 and MnSb, to lithiated fcc structures may ultimately preclude their use as electrodes in viable lithium-ion cells.

2.5. The reaction of Li with InSb

The reaction of lithium with InSb is remarkable in that the transition from InSb to Li_3Sb by lithium insertion and indium extrusion occurs with very little change to the fcc Sb array [10]; it expands by only 4.4% (Fig. 8). When the extruded indium is taken into account, the crystallographic electrode volume increases overall by 46.5%. Although such an electrochemical process leads to the pulverization of the InSb crystallites, the result after the first discharge/charge cycle is an electrode with high surface area. It stands to reason, therefore, that if the extruded indium could be deposited in a controlled manner at the surface of the Li_3Sb particles, then it might be possible to engineer an electrode system that operates with high reversibility, particularly because of the strong structural relationship that exists between InSb and Li_3Sb, and because both Li and In can diffuse within the fcc Sb array [21,22]. In practice, however, the metallic indium is extruded as whiskers that can grow up to 15 μm in length (Fig. 9, [23]), a phenomenon that may be linked to the relatively low melting point of indium (157 °C). This exaggerated crystal growth compromises the reversibility of the reaction; in-situ EXAFS studies of Li/InSb cells have shown that after the first charge to 1.2 V, approximately 40% of the indium remains outside the Sb array as metallic indium. Although the precise details of the electrochemical reaction after the first discharge/charge cycle are not yet

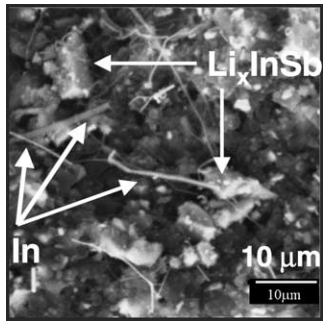

Fig. 9. A transmission electron micrograph of a cycled InSb electrode, showing whiskers of extruded In.

known, the in-situ EXAFS data provide evidence that at the higher potentials, i.e. between 1.2 and 0.7 V, the reaction occurs by lithium insertion into, and indium extrusion from a defect zinc-blende structure without the formation of Sb or Li_2Sb, at least during the early cycles; in this respect, a composition $Li_{1.5}In_{0.5}Sb$ has been observed in high-temperature (400 °C) electrochemical reactions [24]. Lithium reacts with the extruded indium versus Li to form a series of compounds Li_xIn below 650 mV versus Li, thereby breaking up the indium whiskers. The crystal growth of indium and its subsequent reaction with lithium severely compromise the reversibility of the electrochemical InSb to Li_3Sb transformation.

2.6. The reaction of Li with Cu_2Sb

Lithium first reacts with Cu_2Sb to form the lithiated zinc-blende structure Li_2CuSb, which is isostructural with Li_2CuSn (Fig. 4), before transforming to Li_3Sb (Fig. 10) [13]. During this reaction, the fcc Sb array (which is slightly

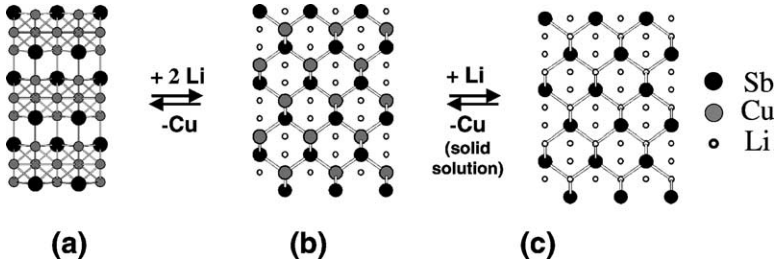

Fig. 10. The transition of (a) Cu_2Sb to (c) Li_3Sb via (b) Li_2CuSb.

distorted in Cu_2Sb) provides a stable framework for lithium and copper. The transition for Cu_2Sb to Li_2CuSb involves the extrusion of 50% of the copper atoms from the structure and a small internal displacement of the remaining Cu atoms to generate the CuSb zinc-blende framework. Further reaction of lithium with Li_2CuSb leads to a $Li_{2+x}Cu_{1-x}Sb$ solid solution with the end-member Li_3Sb at $x = 1$. The Sb array expands by 25% during the transformation of Cu_2Sb to Li_2CuSb, and by a further 13% for the Li_2CuSb to Li_3Sb transition [13]; the total expansion of the electrode, taking the extruded Cu into consideration, is 94%. The reversibility and rate of this reaction is facilitated by the compatibility in the size and charge of the lithium and copper atoms and by the absence of any significant internal displacement of Sb during the transformations. Furthermore, lithium does not alloy with copper to any significant extent at room temperature, thereby restricting this reaction solely to a lithium insertion–copper extrusion process. Apart from an irreversible capacity loss on the initial cycle, this electrode has shown excellent reversibility, yielding 90% of its theoretical capacity (Fig. 11) [13]. The good electrical conductivity of the extruded copper, the apparent absence of copper whiskers and exaggerated grain growth, and the strong structural relationship that exists between the parent Cu_2Sb, the intermediate Li_2CuSb and final product Li_3Sb are considered to be the main reasons for the good electrochemical behavior of this electrode. From a structural viewpoint, therefore, Cu_2Sb has excellent promise as an electrode for lithium batteries. Note that Cu_3Sb, which is isostructural with Li_3Sb, is expected to operate in a similar fashion to Cu_2Sb, but with solid solution behavior throughout the reaction:

$$xLi + Cu_3Sb \rightarrow Li_xCu_{3-x}Sb + Cu(0 < x < 3) \quad (7)$$

with the formation of Li_2CuSb at $x = 2$. Because of its higher copper content, the theoretical capacity of Cu_3Sb (257 mAh/g) is considerably lower than that of Cu_2Sb (323 mAh/g).

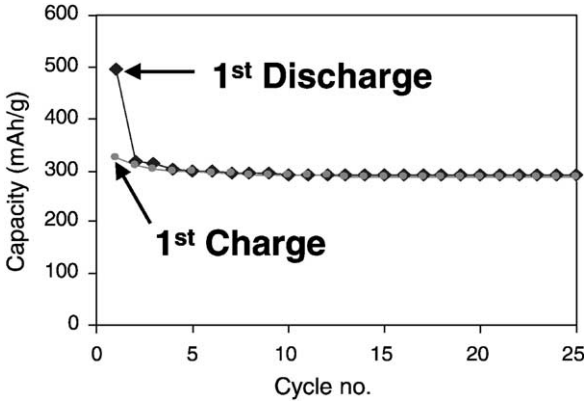

Fig. 11. Capacity versus cycle no. for a Li/Cu_2Sb cell (1.2 to 0 V, 0.2 mA/cm^2).

3. Irreversible capacity loss on the first cycle

One of the major limitations of intermetallic electrodes is that they tend to suffer from a severe irreversible capacity loss on the first cycle. This is particularly evident in the plots of capacity versus cycle number for Cu_2Sb electrodes shown in Fig. 11. For example, the capacity derived from the Cu_2Sb electrode on the initial cycle is 490 mAh/g, which is 52% greater than the theoretical capacity of the electrode (323 mAh/g). Although some capacity may be attributed to an oxidized surface, a surface coating clearly cannot account for all of the surplus capacity. It is therefore believed that much of the initial capacity loss is due to a catalytic reduction of the electrolyte at the surface of the intermetallic electrode as it is pulverized during the initial reaction with lithium. This initial reaction passivates the surface of the intermetallic electrode particles because continued cycling does not lead to any further capacity loss effects of the same magnitude; this behavior is, therefore, similar to the passivation of graphite electrodes that prevents further reaction of the lithiated graphite with the electrolyte at low potentials, thereby allowing the electrode to cycle with high efficiency. In this respect, Cu_2Sb electrodes have been shown to cycle with remarkable efficiency after the first cycle (Fig. 11) [13].

4. An analogy to high-temperature Na/MCl_2 cells (M = Ni, Fe)

The mechanism of lithium insertion-metal extrusion that characterizes the reactions of intermetallic electrodes such as InSb and Cu_2Sb bears a strong resemblance to the manner in which high-temperature sodium/metal chloride "Zebra" cells operate [15–17]. The electrochemical reaction at 300 °C for this system is simply:

$$2Na + MCl_2 \rightarrow 2NaCl + M(M = Ni, Fe) \quad (8)$$

in which Ni is the preferred metal because it provides a higher cell voltage (2.58 V) compared to Fe (2.35 V). The cell construction is based on the earlier sodium–sulfur design [25]. In Zebra cells, the molten sodium electrode is separated from the solid NaCl/Ni electrode by a sodium-ion conducting beta-alumina ceramic membrane (which can therefore be considered to play the same role as the passive film which protects a lithiated graphite electrode in a lithium-ion cell). The NaCl/Ni electrode compartment contains a molten $NaAlCl_4$ electrolyte (melting point = 157 °C) to provide the necessary liquid contact between the sodium ions and the solid electrode particles.

Nickel dichloride has a layered structure in which the Cl^- ions deviate only slightly from ideal cubic-close-packing, i.e. from providing an ideal fcc structure. The electrochemical discharge reaction can, therefore, be considered to occur simply by a process of sodium insertion into, and nickel extrusion from, an invariant close-packed Cl^- framework (predominantly at the particle surface) and is therefore

analogous to the room temperature reactions of lithium with InSb and Cu_2Sb. The Cl^- array expands by 46% (per Cl) atom during the reaction; the electrode expands overall by 64% when the extruded nickel is taken into account. By comparison, the increase in volume of the Sb array of an intermetallic Cu_2Sb electrode is very similar (45% per Sb atom); in this case, the crystallographic electrode volume increases by a larger margin (94%) when the extruded copper is considered.

Zebra cells, like lithium-ion cells are assembled in the discharged state. The positive electrode initially consists of a NaCl/Ni composite mixture containing surplus nickel to provide an electronically conducting and porous matrix for NaCl and the $NaAlCl_4$ electrolyte; the capacity of Zebra cells is therefore controlled by the amount of NaCl in the initial cell. Cells must be cycled between fixed voltage limits, typically between 2.7 and 2.2 V to prevent the formation of trivalent nickel, acidic $AlCl_3$ and chlorine on overcharge and the reduction of the $NaAlCl_4$ electrolyte on overdischarge. Despite this voltage control, early $Na/NiCl_2$ cells lost capacity rapidly because of the pronounced crystal growth of nickel as it was extruded from the $NiCl_2$ electrode structure during discharge, which is analogous to the capacity loss of Li/InSb cells caused by the crystal growth of extruded In. This problem was successfully overcome in Zebra cells by adding approximately 5% sulfur to the positive electrode, which resulted in very fine and highly dispersed Ni particulates in the supporting nickel matrix [26]. Fully engineered Zebra cells, which have been designed to accommodate the volumetric expansion of the electrodes on either side of the beta-alumina ceramic membrane have been cycled with 100% coulombic efficiency and have demonstrated outstanding cycle life [27].

5. Concluding remarks

Room-temperature lithium insertion–metal displacement reactions with intermetallic compounds mimic the high temperature reaction of sodium/metal chloride (Zebra) cells. The strong crystallographic relationship between the structures of the charged and discharged electrodes, particularly those with an invariant fcc host array is believed to contribute to their excellent reversibility, despite expansions of up to 50% of the host array and the extrusion of a metal from the lattice. Such electrochemical reactions, which occur predominantly at the surface of the electrode particles, pulverize the particles, thereby providing systems with high surface area and improved reaction kinetics. The challenge that remains is to devise methods to engineer and design lithium-ion cells and chemistries to capitalize on these features. Following the model of Zebra cells, this should be possible, in principle. Key to the success will be the maintenance of electronic contact between the electrochemically pulverized particles, the choice of a suitable electrolyte, control of grain growth, and a flexible cell design to accommodate the volume changes at the negative electrode.

Acknowledgements

Financial support from the Office of Basic Energy Sciences and from the Office of Advanced Automotive Technologies of the US Department of Energy, and from the Foundation for Environmental Strategic Research (MISTRA), Sweden is gratefully acknowledged.

References

[1] R.A. Huggins, in: J.O. Besenhard (Ed.), Handbook of Battery Materials, Part III.1, Wiley/VCH, Wienheim, Germany, 1999, p. 359.
[2] Y. Idota, T. Kubota, A. Matsufuji, Y. Maekawa, T. Miyasaka, Science 276 (1997) 570.
[3] I.A. Courtney, J.R. Dahn, J. Electrochem. Soc. 144 (1997) 2045.
[4] O. Mao, R.A. Dunlap, J.R. Dahn, J. Electrochem. Soc. 146 (1999) 405.
[5] R. Alacantara, F.J. Fernandez-Madrigal, P. Lavela, J.L. Tirado, J.C. Jumas, J. Olivier-Fourcade, J. Mater. Chem. 9 (1999) 2517.
[6] I. Rom, M. Wachtler, I. Papst, M. Schmied, J.O. Besenhard, F. Hofer, M. Winter, Solid State Ionics 143 (2001) 329.
[7] J. Yang, Y. Takeda, N. Imanishi, J.Y. Xie, O. Yamamoto, Solid State Ionics 133 (2000) 189.
[8] K.D. Kepler, J.T. Vaughey, M.M. Thackeray, Electrochem. Solid State Lett. 2 (1999) 307.
[9] L.M.L. Fransson, E. Norstrom, K. Edstrom, L. Haggstrom, J.T. Vaughey, M.M. Thackeray, J. Electrochem. Soc. 149 (2002) A736.
[10] C.S. Johnson, J.T. Vaughey, M.M. Thackeray, T. Sarakonsri, S.A. Hackney, L. Fransson, K. Edström, J.O. Thomas, Electrochem. Comm. 2 (2000) 595.
[11] K.C. Hewitt, L.Y. Beaulieu, J.R. Dahn, J. Electrochem. Soc. 148 (2001) A402.
[12] H. Tostmann, A.J. Kropf, C.S. Johnson, J.T. Vaughey, M.M. Thackeray, Phys. Rev. B., in press.
[13] L.M.L. Fransson, J.T. Vaughey, R. Benedek, K. Edstrom, J.O. Thomas, M.M. Thackeray, Electrochem. Comm. 3 (2001) 317.
[14] L.M.L. Fransson, J.T. Vaughey, K. Edstrom, M.M. Thackeray, J. Electrochem. Soc., in press.
[15] J. Coetzer, J. Power Sources 18 (1986) 377.
[16] K.T. Adendorff, M.M. Thackeray, J. Electrochem. Soc. 135 (1988) 2121.
[17] R.C. Galloway, J. Electrochem. Soc. 134 (1987) 256.
[18] M.M. Thackeray, J. Electrochem. Soc. 142 (1995) 2558.
[19] M. Winter, J.O. Besenhard, M.E. Spahr, P. Novak, Adv. Mater. 10 (1998) 725.
[20] J.B. Clark, J.W. Hastie, L.H.E. Kihlborg, R. Metselaar, M.M. Thackeray, Pure Appl. Chem. 66 (1994) 577.
[21] T. Takabatake, H. Ikari, Y. Uyeda, Jpn. J. Appl. Phys. 5 (1966) 839.
[22] V.M. Kozlov, V. Agrigento, G. Mussati, L.P. Bicelli, J. Alloys Compd. 288 (1999) 255.
[23] T. Sarakonsri, Ph.D. Thesis, Michigan Technological University, 2002.
[24] W. Sitte, W. Weppner, Z. Naturforsch. 42a (1987) 1.
[25] J.L. Sudworth, R. Tilley, The Sodium Sulfur Battery, Chapman and Hall, London, 1985.
[26] R.J. Bones, D.A. Teagle, S.D. Brooker, F.L. Cullen, J. Electrochem. Soc. 136 (1989) 1274.
[27] J.L. Sudworth, J. Power Sources 100 (2001) 149.